Rapid Communications

Observation and origin of the Δ manifold in Si:P δ layers

Ann Julie Holt,[1] Sanjoy K. Mahatha,[1] Raluca-Maria Stan,[1] Frode S. Strand,[2] Thomas Nyborg,[2] Davide Curcio,[1] Alex K. Schenk,[2] Simon P. Cooil,[2,3] Marco Bianchi,[1] Justin W. Wells,[2] Philip Hofmann,[1] and Jill A. Miwa[1,*]

[1]*Department of Physics and Astronomy, Interdisciplinary Nanoscience Center (iNANO), University of Aarhus, 8000 Aarhus C, Denmark*

[2]*Department of Physics, Center for Quantum Spintronics, Norwegian University of Science and Technology (NTNU), Trondheim NO-7491, Norway*

[3]*Department of Mathematics and Physics, Aberystwyth University, Aberystwyth SY23 3BZ, United Kingdom*

(Received 19 November 2019; revised manuscript received 3 February 2020; accepted 4 February 2020; published 5 March 2020)

By creating a sharp and dense dopant profile of phosphorus atoms buried within a silicon host, a two-dimensional electron gas is formed within the dopant region. Quantum confinement effects induced by reducing the thickness of the dopant layer, from 4.0 nm to the single-layer limit, are explored using angle-resolved photoemission spectroscopy. The location of theoretically predicted, but experimentally hitherto unobserved, quantum well states known as the Δ manifold is revealed. Moreover, the number of carriers hosted within the Δ manifold is shown to be strongly affected by the confinement potential, opening the possibility to select carrier characteristics by tuning the dopant-layer thickness.

DOI: 10.1103/PhysRevB.101.121402

The process of δ doping is to create a high-density doping profile within a narrow, well-defined region of a semiconductor [1–5]. By creating a δ layer of phosphorus in a silicon host, a strong potential is induced in the dopant layer region, giving rise to a highly conductive two-dimensional electron gas [6,7]. δ layers of this kind are the structural element behind a significant number of intriguing developments towards a scalable silicon-based solid-state quantum computer, such as the first single-atom transistor [8], the narrowest conducting nanowire [9], an atomically precise tunneling junction [10], and the fabrication of spin qubits [11,12]. The arrangement of a single or few phosphorus atoms act as hosts for spin qubits, whereas larger dopant regions form the basis of source, drain, and gate electrodes.

For these reasons, considerable effort has been dedicated to developing a complete understanding of Si:P δ layers, in particular the factors influencing their electronic structure. Due to the challenges of measuring buried electron states, theoretical models based on tight-binding (TB) and density functional theory (DFT) have dominated the field [13–18]. These theoretical calculations predict metallic quantum states forming both at the center and close to the corners of the surface Brillouin zone (SBZ) of Si, known as the Γ and Δ states, respectively. The Γ states are the most occupied, and several of these states are predicted to exist below the Fermi level (E_F), depending on the degree of phosphorus doping [19]. Accurate theoretical predictions of the energy splitting between these states, i.e., the so-called valley splitting, are challenging and have resulted in values ranging from 6 to 270 meV [20], making experimental verification a necessity. Previously, angle-resolved photoemission spectroscopy (ARPES) measurements confirmed the formation of the Γ quantum states at the Brillouin zone (BZ) center [7], as well as a description of their orbital character [21], phonon and impurity interactions [22], and the aforementioned valley splitting of the Γ states [23]. While a comprehensive description of the Γ states is thus underway, the theoretically predicted metallic states closer to the SBZ corners, the so-called Δ manifold, have not been experimentally observed, leaving the theoretical calculations in qualitative disagreement with the observations by ARPES. Since the Δ states are found near the SBZ corners, and fourfold degenerate, they are expected to have a high impact on the density of states at E_F. The presence of additional quantum states near E_F would also have crucial implications for Si:P δ-layer-based qubit systems, since a variety of excited states will be possible by the many configurations of valence electrons within the Δ manifold [24].

In this Rapid Communication, we confirm the existence of the theoretically predicted Δ manifold using high-resolution ARPES. The states are located at the corners of the Si SBZ, i.e., at $\mathbf{k} = [\pm 0.68, \pm 0.68]$ Å^{-1}, determined with an uncertainty of ± 0.02 Å^{-1}. Their symmetry and location is in agreement with theoretical models [13–18], settling the incongruity between theory and experimental measurements. In addition, the effect of quantum confinement is investigated as the P dopant layer is reduced from a 4 nm thickness down to a single-atom-thick layer limit. [Note that we use single-layer (SL) to refer to the single-atom-thick layer limit.] We find that the Γ and Δ states have a qualitatively different response to a modified confinement potential, resulting in a redistribution of carriers between the quantum states. This behavior opens the possibility for selecting carrier characteristics by tuning the dopant-layer thickness; a capability which could be capitalized on to enhance the performance of atomic-scale devices constructed from Si:P δ layers.

Three adjacent three-dimensional (3D) BZs of bulk Si are illustrated in Fig. 1(a). In the 3D BZ at the forefront, the six

*miwa@phys.au.dk

 ©2020 American Physical Society

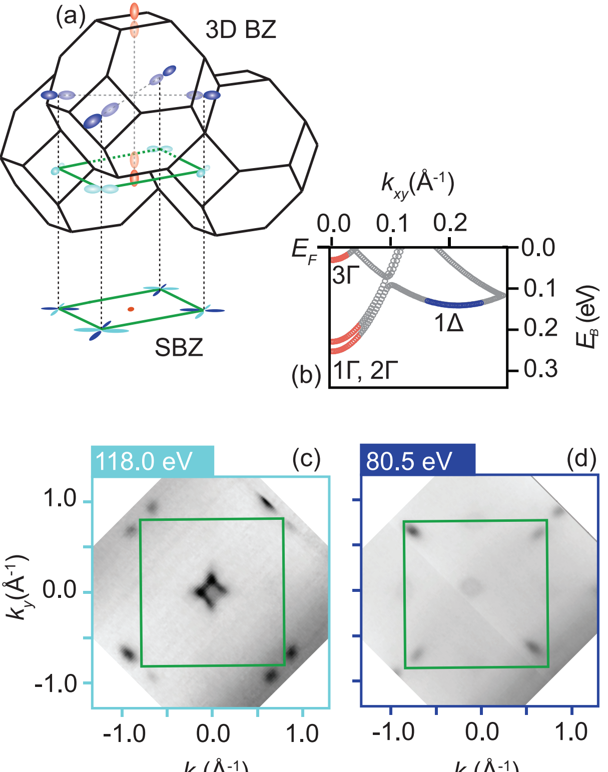

FIG. 1. (a) Projection diagram for a highly confined δ layer. Out-of-plane CBM valleys (red) are projected onto the SBZ center, whereas in-plane CBM valleys (blue) are projected close to the SBZ corners. (b) TB band structure calculation predicting the formation of quantum well states (adapted from Mazzola *et al.* [19]). The most occupied bands (Γ states) originate from confinement of the out-of-plane CBMs, whereas the in-plane CBMs result in shallow Δ states. (c) Constant energy surface at E_F acquired with 118.0 eV and (d) 80.5 eV photons measured on a sample created with a 4 nm δ layer. By combining the intensity of the two spectra all the quantum states depicted in (a) are accounted for in the ARPES data.

conduction band minima (CBMs) are shown. Projecting the 3D BZ and the electronic structure onto the (001) surface results in a square SBZ (green) and CBM-derived electron pockets near the center and the corners of the SBZ. The reduced BZ, shown in Fig. 1(b), is calculated using an empirical $sp^3d^5s^*$ TB model coupled with the Poisson equation for a 2×2 supercell, thus folding the band structure into a smaller BZ. The appropriate unfolding of the bands is explained further in the Supplemental Material Note 1 [25]. The modeled band structure is adapted from Mazzola *et al.* [19], which follows the calculations described in Lee *et al.* [15]. Several confined bands are predicted to appear below E_F, conveniently available for photoemission spectroscopy. The most occupied quantum bands, referred to as the Γ states, arise from the out-of-plane CBMs (red), projected onto the zone center. The Γ states are split because of the formation of bonding and antibonding states as they end up at the same $k_\parallel$. Projection of the in-plane CBMs (blue) result in quantum states appearing close to the SBZ corners, known as the Δ manifold. Each 1Δ state is located at a distinct value of $k_\parallel$ and therefore not split in energy.

Fabrication of Si:P δ-layer samples was made following a known procedure, which yields a $\frac{1}{4}$ monolayer of P dopants on a clean Si(001) surface buried beneath epitaxially grown Si [7,21,23]. In short, a clean (2×1) reconstructed Si(001) surface was obtained by outgassing the substrate to 650 °C for several hours followed by a flash anneal to 1200 °C. The δ layer was created by exposing a reconstructed Si surface to phosphine (PH_3) gas at a pressure of 5×10^{-9} mbar for 5 min with the substrate held at room temperature. The adsorbed hydrogen was subsequently removed by a rapid anneal to 380 °C for 30 s. (We note that the Si surface state and its influence on the measured δ-layer states have been previously measured and commented on in Ref. [7].) Thicker dopant layers were grown by codeposition of PH_3 (i.e., the P dopant source) and Si to produce samples with a dopant concentration on par with the SL case (see Mazzola *et al.* [19] for details). In this work, the dopant layers were buried beneath 1.5 ± 0.5 nm of epitaxial Si by sublimation from a clean Si source. ARPES measurements were acquired at the SGM3 beamline at the ASTRID2 synchrotron (Aarhus, Denmark). During data acquisition the sample was held at room temperature, and the measurements were obtained using a PHOIBOS 150 hemispherical analyzer (SPECS GmbH) with the energy and angular resolutions set to 30 meV and 0.2°, respectively [26].

ARPES measurements showing constant binding energy slices at E_F for a Si:P δ layer with a 4.0-nm-thick dopant layer are presented in Figs. 1(c) and 1(d). The measurements were acquired with a photon energy of 118.0 and 80.5 eV, respectively. These photon energies enabled the whole SBZ to be captured. In accordance with previous reports, the Γ states are observed as intense features appearing at the center of the SBZ. The shape of the 1Γ Fermi contour is highly anisotropic in comparison to 2Γ; the bands are flatter in the k_x and k_y directions than in the k_{xy} direction [13,15,23]. In addition to the dominant Γ states, other electron states are also clearly present close to the SBZ corners. These states are assigned to the Δ manifold, and appear in the positions predicated by theory. Even though all these predicted states are observed [see Figs. 1(c) and 1(d)], they are not all observed at the same photon energy. The reason for this deviation is that the quantum confined states still retain some of their $k_\perp$ character and their ARPES signal is very weak unless they are resonantly excited [21].

As the 3D BZ of Si [see Fig. 1(a)] is a truncated octahedron, the nearest-neighboring 3D BZ is shifted in the $k_\perp$ direction. This shift makes the Δ states appear in a pairwise fashion at specific values of $k_\perp$ in the extended BZ scheme, and their enhanced intensity is therefore obtained pairwise at separate photon energies. In the ARPES measurement presented in Fig. 1(c), there are no Δ states within the first SBZ. A pair of Δ states is, however, visible near each of the SBZ corners but located within the adjacent zones. By reducing the photon energy from 118.0 to 80.5 eV [see Fig. 1(d)], the other pair of Δ states is visible. Together, the two data sets account for all the predicted quantum well states.

The effect of quantum confinement may be investigated by varying the thickness of the dopant layer. We find that decreasing the dopant-layer thickness from 4.0 nm down to a SL drastically alters the properties of the quantum states. Measurements obtained from samples with different

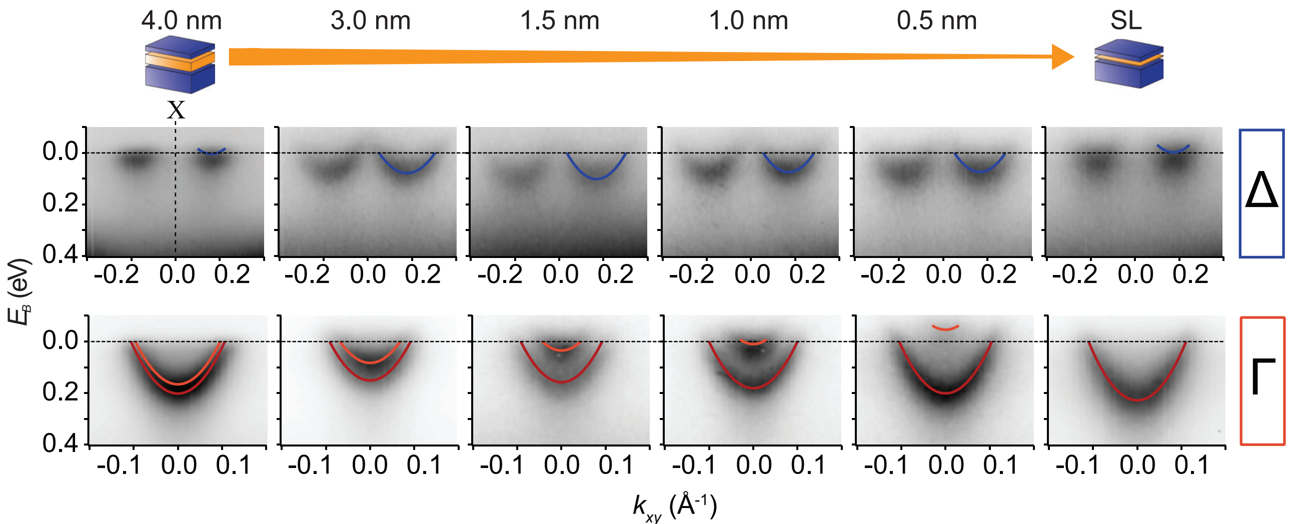

FIG. 2. Energy dispersion showing the development of the 1Δ states as the dopant-layer thickness is reduced (upper row). Corresponding development for the Γ states (lower row). The measurements are acquired with 44.0 and 37.0 eV photons for the Δ and Γ states, respectively. As the confinement increases, the fitted bands of the Γ states separate in energy, whereas the 1Δ band initially moves closer to 1Γ in terms of energy, before reversing this behavior upon reaching a dopant-layer thickness of 1.5 nm. The k_{xy} values for the Δ states (upper panel) are given relative to the SBZ corner.

dopant-layer thicknesses are presented in Fig. 2. The Δ states are shown in the upper panels, while the lower panels show the corresponding Γ states. Note that the k_{xy} values for the Δ states (upper panel) are given relative to the SBZ corner located at $\mathbf{k} = [0.82, -0.82]$ Å^{-1}. The dispersion of the bands is determined by a two-dimensional (2D) fit of the full ARPES spectra, allowing polynomial dispersion up to the third degree for the bare bands. This is a powerful fitting procedure, where one can compare the entire E- and k-dependent data set to a resolution-broadened model of the spectral function [22,27–30]. Further information regarding the 2D fitting process can be found in the Supplemental Material Note 2 [25].

Two parabolic bands are used to represent the Γ states (red and orange). The most occupied band hosts both the 1Γ and 2Γ states, and the less occupied band is assigned to the 3Γ state [19]. As the confinement increases the bands separate in energy, and the induced splitting between them becomes more pronounced. Upon reaching the SL limit 3Γ is pushed completely above E_F, resulting in a lower estimate between the two parabolic bands of 230 meV for describing the energy splitting. As the Γ states are forced to split apart in terms of energy, the increased confinement also affects the binding energy of the Δ states (see upper panels of Fig. 2), relative to that of the most occupied Γ band. This separation, however, is not monotonically increasing. Experiencing an increase in confinement potential, the Δ states first shift closer to 1Γ in terms of energy, before the opposite behavior is instigated upon reaching a confinement exceeding that produced by a 1.5-nm-thick dopant layer.

The divergent dependency on dopant-layer thickness between the separate quantum well bands results in a change of the relative number of carriers within each band, as well as the total number of carriers. The carrier density in the dopant-layer systems is estimated from the occupancy of the bands and presented in Table I. At E_F, the constant energy contour of 1Δ is assumed to be elliptical, with an estimated ratio of 1:2.17 between the short and long axis. A fourfold sinusoidal shape is used to describe the Fermi contour of 1Γ, where the ratio between the short and long radius is estimated to be 1:1.48, whereas 2Γ and 3Γ are assumed to be isotropic. The shape of these contours is based on the work presented in Mazzola *et al.* [19] and the quoted ratios are based on an average determined from constant energy slices, acquired at E_F, for the different δ-layer thicknesses.

For the SL doping limit, the electron carrier density is estimated to be $n_{SL} = 5.0 \times 10^{13}$ e$^-$/cm^2, well above the insulator-to-metal transition [31] and in agreement with ear-

TABLE I. Total carrier density estimation for the different δ-layer systems together with the relative distribution of carriers within each band. The carrier densities are determined within a maximum absolute uncertainty of 3×10^{13} e$^-$/cm^2.

Dopant layer thickness (nm)	Total carrier density (e$^-$/cm^2)	Distribution of carriers (%)			
		1Γ	2Γ	3Γ	1Δ
SL	5×10^{13}	61	39	0	0
0.5	8×10^{13}	33	21	0	46
1.0	8×10^{13}	30	20	4	46
1.5	9×10^{13}	24	15	3	58
3.0	9×10^{13}	24	15	8	53
4.0	6×10^{13}	44	28	23	5

lier transport studies [32–34]. For this system, 1Γ and 2Γ are solely responsible for hosting electron transport at zero temperature, which may explain the previous elusiveness of the Δ manifold. The 1Δ states are, however, located close enough to E_F to be thermally populated at room temperature.

The δ-layer system with a 4.0-nm-thick dopant layer shows a similar distribution, in the sense that the electron carriers are primarily hosted by the Γ bands, located at the BZ center. Simplified transport calculations only include the Γ bands, and may therefore serve as a good model for both these situations. For the intermediate dopant-layer thicknesses, however, the carrier distribution changes significantly. The carrier contribution from the 1Δ states can no longer be neglected, since these are found to account for over 46% of the electron carriers in all of the studied intermediate systems, i.e., 0.5–3.0 nm thicknesses. Although the 1Δ band always appears less occupied than 1Γ and 2Γ, the fourfold degeneracy compensates for the shallow binding energy, giving the Δ manifold a high impact on the density of states at E_F. It is even shown that for a system with a 1.5-nm-thick dopant layer the 1Δ states are contributing with 58% of the total carrier density. In order to obtain an accurate description of the electronic properties of Si:P δ-layer-based devices, it is, therefore, crucial to include the Δ manifold in any model.

In summary, the existence of the theoretically predicted Δ manifold was verified. The location of these states was shown to be in agreement with DFT and TB calculations, giving strength to the developed models. The energy separation between the two parabolic bands used to describe the Γ bands was found to increase monotonically with confinement, reaching a separation of at least 230 meV for the SL limit. The revealed Δ manifold was shown to accommodate a significant portion of electron carriers. In particular, the Δ manifold hosts over 46% of the electron carriers for all systems with dopant-layer thicknesses between the SL and 4.0 nm. Notably, in the 1.5-nm-thick dopant-layer sample, 58% of the carriers are supplied by the Δ manifold. Such a significant contribution to the carrier statistics demands the inclusion of these states for obtaining an accurate model of any future device based on this platform. In fact, the influence of these states has already been suspected in a study by Fuechsle *et al.* [24], where the presence of the Δ manifold would explain the observed electron states generated in a quantum dot system. The experimental verification and the careful investigation of these states are thus an important step towards obtaining an accurate description of δ-layer-based devices and contribute to the development of a working quantum computer.

This work was supported by the Danish Council for Independent Research, Natural Sciences under the Sapere Aude program (Grants No. DFF-4002-00029 and No. DFF-6108-00409), the Aarhus University Research Foundation, and the VILLUM FONDEN via the Centre of Excellence for Dirac Materials (Grant No. 11744), the Research Council of Norway through its Centres of Excellence funding scheme, Project No. 262633, “QuSpin,” and through the Fripro program, Project No. 250985 “FunTopoMat” and Project No. 262339 “NEAT”. Affiliation with the Centre for Integrated Materials Research (iMAT) at Aarhus University is gratefully acknowledged. We also thank C.-Y. Chen and R. Rahman for carrying out the TB calculation presented in this work.

[1] A. D. Jewell, M. E. Hoenk, A. G. Carver, and S. Nikzad, J. Vac. Sci. Technol. A **36**, 061513 (2018).

[2] H. Gossmann, E. F. Schubert, D. J. Eaglesham, and M. Cerullo, Appl. Phys. Lett. **57**, 2440 (1990).

[3] G. Gramse, A. Kölker, T. Lim, T. J. Z. Stock, H. Solanki, S. R. Schofield, E. Brinciotti, G. Aeppli, F. Kienberger, and N. J. Curson, Sci. Adv. **3**, e1602586 (2017).

[4] T. Škereň, S. Köster, and A. Fuhrer, arXiv:1912.06188.

[5] T. Škeren, N. Pascher, A. Garnier, P. Reynaud, E. Rolland, A. Thuaire, D. Widmer, X. Jehl, and A. Fuhrer, Nanotechnology **29**, 435302 (2018).

[6] C. M. Polley, W. R. Clarke, J. A. Miwa, M. Y. Simmons, and J. W. Wells, Appl. Phys. Lett. **101**, 262105 (2012).

[7] J. A. Miwa, P. Hofmann, M. Y. Simmons, and J. W. Wells, Phys. Rev. Lett. **110**, 136801 (2013).

[8] M. Fuechsle, J. A. Miwa, S. Mahapatra, H. Ryu, S. Lee, O. Warschkow, L. C. L. Hollenberg, G. Klimeck, and M. Y. Simmons, Nat. Nanotechnol. **7**, 242 (2012).

[9] B. Weber, S. Mahapatra, H. Ryu, S. Lee, A. Fuhrer, T. C. G. Reusch, D. L. Thompson, W. C. T. Lee, G. Klimeck, L. C. L. Hollenberg *et al.*, Science **335**, 64 (2012).

[10] M. G. House, E. Peretz, J. G. Keizer, S. J. Hile, and M. Y. Simmons, Appl. Phys. Lett. **104**, 113111 (2014).

[11] M. Koch, J. G. Keizer, P. Pakkiam, D. Keith, M. G. House, E. Peretz, and M. Y. Simmons, Nat. Nanotechnol. **14**, 137 (2019).

[12] Y. Wang, C.-Y. Chen, G. Klimeck, M. Y. Simmons, and R. Rahman, Sci. Rep. **6**, 31830 (2016).

[13] D. J. Carter, O. Warschkow, N. A. Marks, and D. R. McKenzie, Phys. Rev. B **79**, 033204 (2009).

[14] D. J. Carter, N. A. Marks, O. Warschkow, and D. R. McKenzie, Nanotechnology **22**, 065701 (2011).

[15] S. Lee, H. Ryu, H. Campbell, L. C. L. Hollenberg, M. Y. Simmons, and G. Klimeck, Phys. Rev. B **84**, 205309 (2011).

[16] D. W. Drumm, L. C. L. Hollenberg, M. Y. Simmons, and M. Friesen, Phys. Rev. B **85**, 155419 (2012).

[17] D. J. Carter, O. Warschkow, N. A. Marks, and D. R. McKenzie, Phys. Rev. B **87**, 045204 (2013).

[18] J. S. Smith, J. H. Cole, and S. P. Russo, Phys. Rev. B **89**, 035306 (2014).

[19] F. Mazzola, C.-Y. Chen, R. Rahman, X.-G. Zhu, C. M. Polley, T. Balasubramanian, P. D. C. King, P. Hofmann, J. A. Miwa, and J. W. Wells, arXiv:1904.10929.

[20] D. W. Drumm, A. Budi, M. C. Per, S. P. Russo, and L. C. L Hollenberg, Nanoscale Res. Lett. **8**, 111 (2013).

[21] F. Mazzola, M. T. Edmonds, K. Høydalsvik, D. J. Carter, N. A. Marks, B. C. C. Cowie, L. Thomsen, J. Miwa, M. Y. Simmons, and J. W. Wells, ACS Nano **8**, 10223 (2014).

[22] F. Mazzola, C. M. Polley, J. A. Miwa, M. Y. Simmons, and J. W. Wells, Appl. Phys. Lett. **104**, 173108 (2014).

[23] J. A. Miwa, O. Warschkow, D. J. Carter, N. A. Marks, F. Mazzola, M. Y. Simmons, and J. W. Wells, Nano Lett. **14**, 1515 (2014).
[24] M. Fuechsle, S. Mahapatra, F. A. Zwanenburg, M. Friesen, M. A. Eriksson, and M. Y. Simmons, Nat. Nanotechnol. **5**, 502 (2010).
[25] See Supplemental Material at http://link.aps.org/supplemental/10.1103/PhysRevB.101.121402 for details regarding band structure unfolding and the 2D fitting process.
[26] S. Hoffmann, C. Schultz, Z. Li, and P. Hofmann, Nucl. Instrum. Methods Phys. Res., Sect. A **523**, 441 (2004).
[27] I. A. Nechaev, M. F. Jensen, E. D. L. Rienks, V. M. Silkin, P. M. Echenique, E. V. Chulkov, and P. Hofmann, Phys. Rev. B **80**, 113402 (2009).
[28] F. Mazzola, J. W. Wells, R. Yakimova, S. Ulstrup, J. A. Miwa, R. Balog, M. Bianchi, M. Leandersson, J. Adell, P. Hofmann *et al.*, Phys. Rev. Lett. **111**, 216806 (2013).
[29] F. Andreatta, H. Rostami, A. G. Cabo, M. Bianchi, C. E. Sanders, D. Biswas, C. Cacho, A. J. H. Jones, R. T. Chapman, E. Springate, P. D. C. King, J. A. Miwa, A. Balatsky, S. Ulstrup, and P. Hofmann, Phys. Rev. B **99**, 165421 (2019).
[30] P. Hofmann, I. Y. Sklyadneva, E. D. L. Rienks, and E. V. Chulkov, New J. Phys. **11**, 125005 (2009).
[31] S. V. Kravchenko and M. P. Sarachik, Rep. Prog. Phys. **67**, 1 (2004).
[32] K. E. J. Goh, L. Oberbeck, M. Y. Simmons, A. R. Hamilton, and M. J. Butcher, Phys. Rev. B **73**, 035401 (2006).
[33] K. E. J. Goh, M. Y. Simmons, and A. R. Hamilton, Phys. Rev. B **77**, 235410 (2008).
[34] S. R. McKibbin, W. R. Clarke, A. Fuhrer, and M. Y. Simmons, J. Cryst. Growth **312**, 3247 (2010).